Fabrication of Polymer-Gadolinium (III) Complex Nanomicelle from Poly(ethylene glycol)-Polysuccinimide Conjugate and Diethylenetriaminetetraacetic Acid-Gadolinium as Magnetic Resonance Imaging Contrast Agents

Wei-Lu Zhang,[1,2] Da-Wei Yong,[1] Jin Huang,[1,3] Jia-Hui Yu,[1] Shi-Yuan Liu,[4] Ming-Xia Fan[5]

[1]*Institutes for Advanced Interdisciplinary Research, East China Normal University, Shanghai 200062, People's Republic of China*
[2]*Department of Applied Chemistry, College of Chemistry and Materials Science, Wenzhou University, Wenzhou 325035, Zhejiang Province, People's Republic of China*
[3]*College of Chemical Engineering, Wuhan University of Technology, Wuhan 430070, People's Republic of China*
[4]*Department of Diagnostic Imaging, Changzheng Hospital, Shanghai 200003, People's Republic of China*
[5]*Shanghai Key Laboratory of Magnetic Resonance, East China Normal University, Shanghai 200062, People's Republic of China*

Received 1 August 2010; accepted 27 September 2010
DOI 10.1002/app.33464
Published online 23 December 2010 in Wiley Online Library (wileyonlinelibrary.com).

ABSTRACT: Methoxy poly (ethylene glycol)-*graft*-α, β-poly (aspartic acid) derivatives (mPEG-*g*-PAA-N_3) were synthesized by sequential ring-opening reaction of polysuccinimide (PSI) with mPEG-NH_2 (MW: 2000 Da), and 1-azido-3-aminopropane, respectively. Then N^2-(hex-5-yne)-diethylenetriamine-tetra-*t*-butylacetate (DTTA-der) was conjugated to mPEG-*g*-PAA-N_3 by click cycloaddition. After deprotection of carboxylic groups, mPEG-*g*-PAA-DTTA macromolecular ligands were obtained. MPEG-*g*-PAA-(DTTA-Gd) complex nanomicelles were fabricated from mPEG-*g*-PAA-DTTA and Gadolinium chloride. The formation of nanomicelles was confirmed by fluorescence spectrophotoscopy and particle size measurements. It was found that all the nanomicelles showed spherical shapes with core-shell structures and narrow size distributions. Their sizes ranged from 50 to 80 nm, suggesting their passive targeting potential to tumor tissue. With the increase of graft degree (GD) of mPEG, the sizes of mPEG-*g*-PAA-(DTTA-Gd) nanomicelles showed a tendency to decrease. Compared with gadopentetate dimeglumine (Gd-DTPA), mPEG-*g*-PAA-(DTTA-Gd) nanomicelles showed essential decreased cytotoxicity to KB cell line and enhanced T_1-weighted signal intensity, especially at low concentration of gadolinium (III), suggesting their great potentials as magnetic resonance imaging contrast agents. © 2010 Wiley Periodicals, Inc. J Appl Polym Sci 120: 2596–2605, 2011

Key words: polymer-gadolinium (III) complex; nanomicelle; magnetic resonance imaging; Click reaction; cytotoxicity; contrast agent

INTRODUCTION

Magnetic resonance imaging (MRI) is one of the most powerful diagnostic imaging tools in medicine, because it provides not only images for clinic diagnosis but also functional information in a noninvasive and real-time monitoring manner.[1] Now, about 30% of all the MRI diagnoses are performed with the aid of Gd-based MRI contrast agent.[2] This contrast agent is a diagnostic agent that could be administered to a patient to enhance the image contrast between normal and diseased tissues and indicate the status of organ function or blood flow.[3] Several kinds of low molecular weight MRI contrast agents based on Gd-diethylenetriaminepentaacetate (Gd-DTPA) or Gd-tetraazacyclododecanetetraacetic acid (Gd-DOTA) have been widely used in clinical diagnosis of tumors.[4] However, these low molecular weight contrast agents have their inherent problems such as short half-life in blood, lack of specificity to tumor tissues for diagnosis, and low resolution rate results in not well enough imaging contrast effect. To achieve the early diagnosis of tumors, research efforts have been made in developing macromolecular MRI contrast agents by the conjugation of DTPA or other chelating units with polymers. Poly (ethylene glycol) (PEG),[5] dextran,[6] poly (L-lysine),[7] poly (glutamic acid),[8] disulfide-based biodegradable

Correspondence to: J.-H. Yu (yujh109@yahoo.com.cn); M.-X. Fan (mxfan@phy.ecnu.edu.cn)
Contract grant sponsor: International Corporation Project of Shanghai Municipality Commission; contract grant number: 10410710000 and 09540709000.
Contract grant sponsor: Shanghai Municipality Commission for Special Project of Nanometer Science and Technology; contract grant number: 0952nm05300.
Contract grant sponsor: Self-Determined and Innovative Research Funds; contract grant number: WUT 2010-II-022.

synthetic polymers,[9] and dendrimers[10,11] have been investigated as the carriers of gadolinium complexes. The improving MRI contrast agents via macromolecular conjugation showed great promise for enhancing contrast, sensitivity, and diagnostic imaging time.[12]

However, the greatest risk from MRI contrast agents is the release of gadolinium from the chelate, which can lead to nephrogenicsystemicfibrosis or acute metal toxicity. To decrease the toxicity of contrast agents and enhance their specificity to tumor tissues, very recently, much attention has been paid to polymeric nanomicelle MRI contrast agents.[13,14] Because well-designed polymeric nanomicelle MRI contrast agents can be dissociated into copolymer chains, a low risk of chronic toxicity is expected due to the complete excretion of copolymer chains by kidney filtration over a long time period. In addition, polymeric nanomicelle MRI contrast agents exhibit a preferential pharmacokinetic profile in a defined time period required for the targeting of tumors. A strong advantage of the polymeric micelle MRI contrast agents is their high structural stability in the bloodstream and their very small size, being in a range of 10–100 nm. This size range is preferable for the passive targeting of solid tumors by means of the enhanced permeability and retention effect.[15]

Previous reports showed that copolymer with metal ion could be fabricated into polymer-metal ion complex nanomicelle and the metal-complexed polymeric micelles in aqueous media maybe useful in the biomedical field as carriers of diagnostic metals and metal-complex drugs.[16] In that way, a simple mixing of *cis*-dichlorodiammine platinum (II) (CDDP) with poly (ethylene glycol)-poly (α, β-aspartic acid) copolymer in aqueous media led to a spontaneous formation of narrowly distributed core-shell nanomicelles, where the cores of polycarboxylate-CDDP complexes were surrounded by a corona shell of hydrophilic poly (ethylene glycol) chains.[17] With this strategy, graft copolymer-metal ion complex nanomicelles were also obtained by mixing mPEG-*g*-α, β-poly [(*N*-amino acidyl)-DL-aspartamide] and CDDP in our group.

Herein, to develop gadolinium (III)-based polymeric nanomicelle MRI contrast agents, poly (ethylene glycol)-*graft*-α, β-poly (aspartic acid) (mPEG-*g*-PAA) derivatives were synthesized by sequential ring-opening reaction of polysuccinimide (PSI) with mPEG-NH_2 (*M*w: 2000 Da), and 1-azido-3-aminopropane, respectively. Then N^2-(hex-5-yne)-diethylenetriamine-tetra-*t*-butylacetate (DTTA-der) was conjugated to mPEG-*g*-PAA derivatives by click cycloaddition to yield the macromolecular ligands of mPEG-*g*-PAA-DTTA. MPEG-*g*-PAA-(DTTA-Gd) complex nanomicelles were fabricated from mPEG-*g*-PAA-DTTA and gadolinium chloride. The formation of nanomicelles was confirmed by fluorescence spectrophotoscopy, dynamic light scattering (DLS), transmission electron microscopy (TEM), and atomic force microscope (AFM). The *in vitro* image contrast effect and toxicity of mPEG-*g*-PAA-(DTTA-Gd) complex nanomicelles were also evaluated.

EXPERIMENTAL

Materials

α-Methoxy-ω-amino-poly (ethylene glycol) (mPEG-NH_2, MW: 2000) was synthesized according to the literature.[18] 1-azido-3-aminopropane was synthesized according to the literature.[19] N^2-(hex-5-yne)-diethylenetriamine-tetra-*t*-butylacetate (DTTA-der) was synthesized according to the literature.[20] Tetrahydrofuran (THF), ether, *N*, *N*-dimethylformamide (DMF) were purchased from Sinopharm Chemical Reagent Co. DMF was dried overnight with 4 Å molecular sieve and redistilled before use. 3-Chloropropylamine hydrochloride, sodium azide, gadolinium chloride hexahydrate ($GdCl_3{\cdot}6H_2O$), and 3-(4, 5-dimethylthiazol-2-yl)-2, 5-diphenyltetrazolium bromide, MTT) were obtained from Sigma-Aldrich (Shanghai, China).

Measurements

^{1}H-nuclear magnetic resonance (^{1}H-NMR) spectra were recorded with a Bruker Avarice™ 500 NMR spectrometer in d_6-dimethyl sulfoxide (DMSO) at 25°C. The molecular weights of samples were measured with Agilent 1200 gel permeation chromatography (Agilent Technologies, Shanghai, China). Agilent 1200 refractive index detector and aqueous SECstart-up kit were used. Chromatography columns (PL aquagel-OH MIXED columns, Polymer Laboratories, Amherst, MA) were calibrated with poly (ethylene glycol) kit. The column temperature was set at 25°C. Mobile phase was phosphate buffer solution (PBS), and the flow rate was 1.0 mL/min. The particle sizes, size distributions, and zeta potentials (ζ) of polymeric micelles were measured by DLS (Zetasizer Nano ZS, Malvern Instruments, Worcestershire, UK). Fluorescence measurement was performed on a Hitachi F-4500 Fluorescence Spectrophotometer, samples were dissolved in pure water, and pyrene was used as the fluorescent probe. The morphology of the polymeric micelles was observed using AFM (Ai-jian nano-material microscope). A 10 μL of polymeric micelle solution (40 μg/mL) was dropped onto mica plate, and then air dried for 24 h. For TEM measurement, a 10 μL of polymer-gadolinium (III) complex nanomicelle solution of 40 μg/mL was carefully dropped onto clean copper grids, then dried at 50°C for 35 min before imaging on JEM-100C II microscope (LIBRA 120, Carl Zeiss,

Germany). Tests of longitudinal relaxation time (T_1) were performed with a SIEMENS MAGNETOM Trio I-class 3T-MRI. Inductively coupled plasma (ICP) measurements were performed with a Thermo Electron IRIS Intrepid II XSP atomic emission spectrometer (AES) instrument under an argon atmosphere. The samples (1.0 mg) were digested with aqua regia over night to determine the mass content of Gd by using ICP-AES. The optical density (OD) was determined by a BIO-TEK PowerWave XS Microplate Spectrophotometer.

Synthesis of mPEG-*graft*-PSI copolymers (mPEG-*g*-PSI)

Poly (L-succinimide) (PSI) was synthesized according to the previous method, and the molecular weigh was about 19,000 Da.[21] MPEG-*g*-PSI was synthesized by partial ring-opening reaction of PSI with mPEG-NH_2.[22] In a typical reaction procedure, a suitable amount of mPEG-NH_2 (0.5 g, -NH_2: 0.23 mmol) and PSI (0.22 g, 11.5 μmol) were dissolved in DMF, respectively. MPEG-NH_2 solution was slowly dropped into the solution of PSI, and the mixture was stirred at 60°C under nitrogen atmosphere for 48 h. The resultant was precipitated in cold ethyl ether. After filtration, the precipitate was washed several times with THF to remove the unreacted mPEG-NH_2, and dried in vacuum at 30°C for 24 h, yield (0.1 g, 41.4%).

With the change of the molar ratio of succinimide in PSI to mPEG-NH_2, the copolymers with different graft degree (GD) were prepared. The GD of mPEG-*g*-PSI copolymer was defined as the molar ratios of the opened pentacyclic ring in PSI with mPEG-NH_2 to the total amount of pentacyclic ring of PSI. It was calculated from the following equation:

$$\mathrm{GD}(\%) = \frac{S_d}{S_d + S_c} \times 100 \quad (1)$$

where S_c is the integral area of the methyene proton at 5.24 ppm in succinimide units, and S_d is that at 4.17 ppm in the opened pentacyclic rings in the ^{1}H-NMR of mPEG-*g*-PSI.

Synthesis of azido derivative of mPEG-g-PSI (mPEG-*g*-PAA-N_3)

MPEG-*g*-PAA-N_3 was synthesized by full ring-opening reaction of mPEG-*g*-PSI with 1-azido-3-aminopropane according to the following steps. MPEG-*g*-PSI solution (0.1 g, 4.7 μmol) in 5 mL DMF was dropped into excess of 1-azido-3-aminopropane (0.19 g, 1.9 mmol) in 5 mL DMF and stirred under nitrogen atmosphere at 60°C for 48 h. After removal of most of DMF by rotary evaporation, the solution was thoroughly dialyzed using Spectra/Pro membrane (molecular weight cut-off size: 1000 Da) against DMF at room temperature for 24 h. After evaporation of DMF, the final product was labeled as mPEG-*g*-PAA-N_3 with 0.08 g.

Synthesis of mPEG-*g*-PAA-DTTA

MPEG-*g*-PAA-DTTA was synthesized according to following procedure. Briefly, DTTA-der (200.0 mg, -alkynyl: 0.31 mmol) and mPEG-*g*-PAA-N_3 (63.8 mg, 1.84 μmol) were dissolved in 2.0 mL of a mixed solvent (THF/water = 1/1). $CuSO_4{\cdot}5H_2O$ (40 mg, 0.16 mmol, equal to DTTA-der) and sodium ascorbate (31.0 mg, 0.16 mmol) were both charged into the reaction mixture to promote the click coupling reaction using similar conditions developed by Hawker and coworkers.[23] This mixture was stirred briefly at 60°C to promote dispersion, and then stirred at room temperature until the solution became turquoise-blue (after about 8 h), which signified reaction completion. The reaction mixture was then partitioned between water and dichloromethane (10 mL of each) and stirred for 2 min. The dichloromethane layer was retained and washed with a 0.1*M* Na^+ EDTA solution (2 × 10 mL) and ultrapure water (2 × 10 mL), respectively. The organic layer was retained and dried over sodium sulfate and evaporated *in vacuo* to yield a viscous yellow solid (252 mg, 95.4%).

The yellow solid was then redissolved in 2.0 mL of CH_2Cl_2, and 2.0 mL of trifluoroacetic acid (TFA) was added. The mixture solution was kept at room temperature and stirred for 48 h, after which, the TFA/CH_2Cl_2 mixture were removed *in vacuo* to leave viscous oil. Anhydrous ether was added to the oil and allowed to sonicate for 5 min, yielding a white precipitate. The white powder was recovered and dissolved in 2 mL of water and dialyzed extensively against ultrapure water in a 1000 molecular weight cut-off membrane. The purified solution was lyophilized to dryness yielding mPEG-*g*-PAA-DTTA (200 mg) as a fluffy white solid. It should be noted that this product is very hygroscopic and stored in a desiccator.

Preparation of polymer-gadolinium complex based on mPEG-*g*-PAA-DTTA and gadolinium chloride

Polymer-gadolinium complex was prepared according to the method described by Bryson et al.[20] Briefly, mPEG-*g*-PAA-DTTA (23.0 mg, moles of DTTA unit: 3.48×10^{-5} mol) was dissolved in 5 mL of ultrapure water and the solution was adjusted to pH = 7 with sodium bicarbonate. $GdCl_3{\cdot}6H_2O$ (23.4 mg, 6.28×10^{-5} mol) was dissolved in 1 mL of ultrapure water and added to the solution of mPEG-*g*-PAA-DTTA in three separate aliquots. After the addition of each aliquot, the pH was adjusted to a pH between 8 and 9

using 0.1*M* potassium carbonate solution. The mixture was allowed to stir for 30 min, then dialyzed against ultrapure water for 24 h and lyophilized to yield the final product as a fluffy white solid (27.3 mg). The mass percentage content of Gd, theoretically, for each unit containing Gd (98 for unit of PSI + 560 for DTTA + 100 for 1-azido-3-aminopropane + 157 for Gd + 18 for H_2O) was 16.8%.

CMC measurement of mPEG-*g*-PAA-(DTTA-Gd) complex nanomicelles

Critical micelle concentration (CMC) of mPEG-*g*-PAA-(DTTA-Gd) complex nanomicelles in water was determined by fluorescence spectrophotometer. The concentration of pyrene probe in acetone was 6.0×10^{-7} M. In each experiment, 5 μL of pyrene solution in acetone was added to 4 mL of micelle aqueous solution (concentration: 1×10^{-10}–1×10^{-1} mg/mL) and stirred for 24 h until the acetone was completely evaporated before measurement. The ratios of pyrene probe fluorescence intensity at 339 and 337 nm (I_{339}/I_{337}) were calculated and plotted against the concentration logarithm of micelles.

Cell lines and culture

KB cell (human nasopharyngeal cell line) was supplied from Institute of Biochemistry and Cell Biology, Chinese Academy of Sciences, Shanghai. Cells were cultured in RPMI 1640 (Gibco BRL, Paris, France), supplemented with 10% fetal bovine serum (FBS, HyClone, Logan, Utah), streptomycin at 100 μg/mL, and penicillin at 100 Unit/mL. All cells were incubated at 37°C in humidified 5% CO_2 atmosphere. Cells were splitted by using trypsin/EDTA solution when almost confluent.

Cell viability assays

In vitro cytotoxicity of polymer-gadolinium (III) complex nanomicelle to inhibit cells growth was determined by evaluation of the viability of KB cell lines by MTT assay. Briefly, cells were seeded in 96-well plates at an initial density of 1×10^4 cells/well in 200 μL growth medium and incubated for 18–20 h to reach 80% confluency at the time of treatment. Growth medium was replaced with 100 μL fresh serum-free media containing various amounts of the sample (25, 50, 75, 100, 125, 150, 175, and 200 μg/mL). Cells were incubated for 24 and 48 h, respectively. And then, the culture medium was replaced by 100 μL of MTT solution (0.5 mg/mL). After further incubation for 4 h in incubator, 100 μL of DMSO was added to each well to replace the culture medium and dissolve the insoluble formazan-containing crystals. The OD was measured at 570 nm using an automatic BIO-TEK microplate reader (Powerwave XS), and the cell viability was calculated from following equation:

$$\text{Cell viability}(\%) = \frac{\text{OD}_{\text{sample}}}{\text{OD}_{\text{control}}} \times 100 \quad (2)$$

where $\text{OD}_{\text{sample}}$ represents an OD value from a well treated with samples and $\text{OD}_{\text{control}}$ from a well treated with PBS buffer only. Each experiment was carried out in triplicate. Means and corresponding standard deviations (mean ± SD) were shown as results.

In vitro contrast effect evaluation and relaxtivity

In vitro MR imaging was evaluated using an inversion recovery pulse sequence (Siemens Tim 3 T MRI scanner) at 3.0 T. The T_1-weighted MR images of the prepared samples mPEG-*g*-PAA-(DTTA-Gd) and the commercially available contrast agent of Gd-DTPA were obtained in deionized water with Gd concentrations ranging from 1.0×10^{-3} to 0.5×10^{-5} M in vials with an inner diameter of 5 mm. The experimental condition was as follows: TE (echo delay time) = 7.6 ms, TR (recycle time) = 5000 ms, FOV (field of view): 108×180 cm^2. MR images were analyzed with Syngo fastView software. Deionized water was measured as control.

Relaxation rate (r_1) ($r_1 = 1/T_1$) was calculated from a linear least squares fit of the slope of the line obtained from following formula by plotting $1/T_1$ versus Gd concentration in corresponding mPEG-*g*-PAA-(DTTA-Gd) solution.

$$\frac{1}{T_{\text{wat}}} = \frac{1}{T_{\text{obs}}} + r_1 \times [C] \quad (3)$$

where T_{wat} was the relaxation time of water; T_{obs} was the relaxation time of solution of mPEG-*g*-PAA-(DTTA-Gd); and *C* was the corresponding Gd concentration of each mPEG-*g*-PAA-(DTTA-Gd) solution.

RESULTS AND DISCUSSION

Synthesis and characterization of mPEG-*g*-PAA-DTTA

To prepare the micelle-formed MRI contrast agent with Gd, at first, PSI, mPEG-PSI, mPEG-*g*-PAA-N_3, and mPEG-*g*-PAA-DTTA were sequentially synthesized. The overall synthetic route of mPEG-*g*-PAA-DTTA was shown in Scheme 1. MPEG-*g*-PAA-N_3 was initially synthesized through ring-opening of PSI with mPEG-NH_2, then with 1-azido-3-aminopropane.

^{1}H-NMR spectra of PSI, mPEG-PSI, mPEG-*g*-PAA-N_3, and mPEG-*g*-PAA-DTTA were shown in

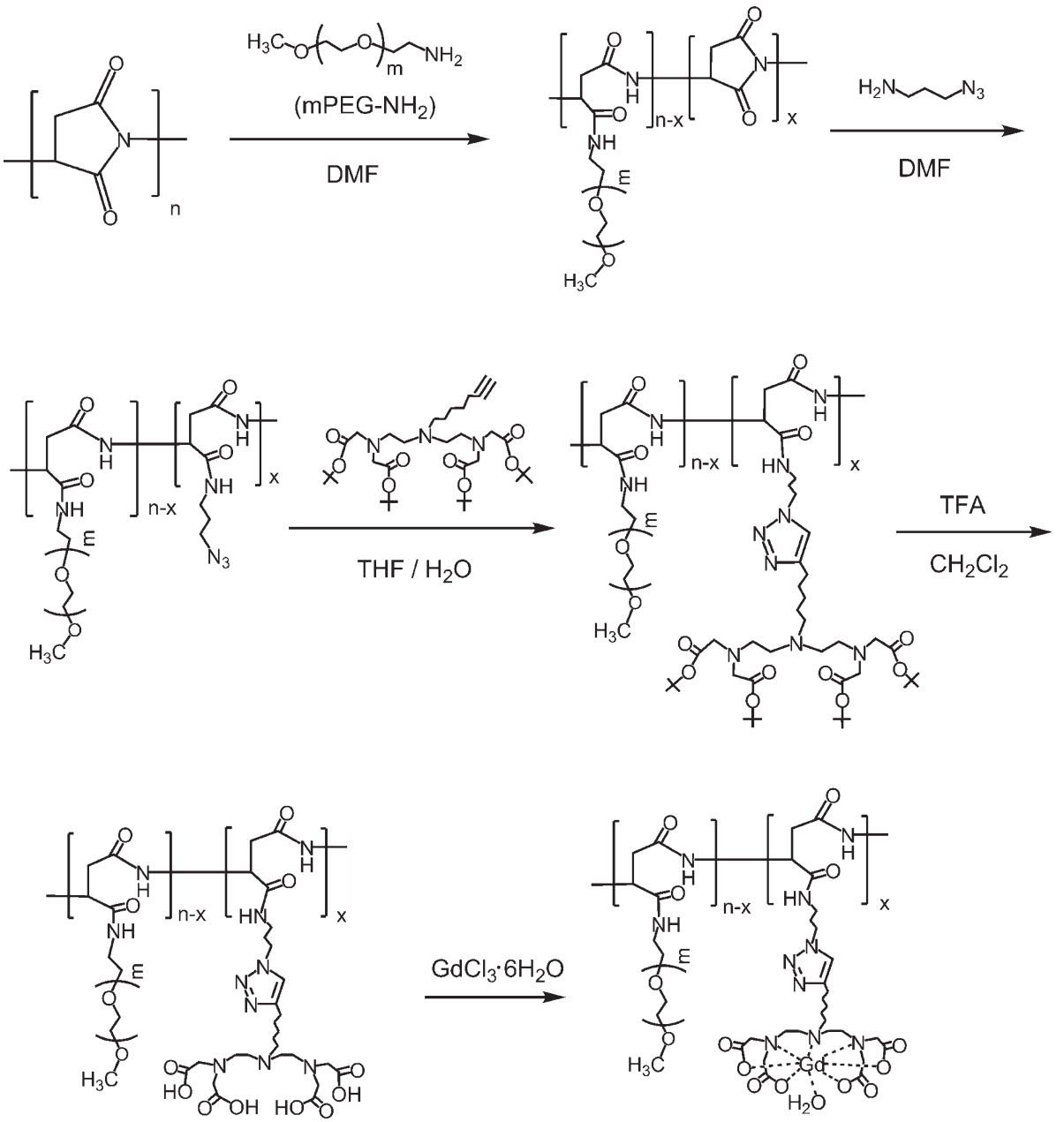

Scheme 1 Synthesis scheme of mPEG-*g*-PAA-(DTTA-Gd).

Figure 1(A–D). The signals at 2.5–3.5 ppm were assigned to the methylene protons (a) and the signals at 5.24 ppm were assigned to the methyne proton (b) of the repeating succinimide unit. The GDs of mPEG-*g*-PSI measured by ^{1}H-NMR were 1.8% and 6.6%, just similar to the theoretic values of 2 and 7%, respectively. The structure of mPEG-*g*-PAA-N_3 and their detail chemical shifts were shown in Figure 1(B). The disappearance of the peak at 5.24 ppm [Fig. 1(B)] clearly indicated that the rings in PSI were thoroughly opened by 1-azido-3-aminopropane. The new signals at 3.42 ppm assigned the methylene triplet (-CH_2N_3) in mPEG-*g*-PAA-N_3 shown in Figure 1(C).

Synthesis and characterization of mPEG-*g*-PAA-(DTTA-Gd)

DTTA used as a chelating agent was combined with mPEG-*g*-PAA-N_3,and Gd was incorporated into the complex. DTTA-der was coupled with mPEG-*g*-PAA-N_3 by click cycloaddition between the alkyno groups in DTTA-der and the azido groups in mPEG-*g*-PAA-N_3. Figure 1(A) showed ^{1}H-NMR analysis data of mPEG-*g*-PAA-DTTA. New signals at 7.32 and 4.25 ppm, corresponding to the triazole proton R_2C = CHR and the methylene group adjacent to the triazole CH_2NR, respectively, which indicated the conjugation of click cycloaddition.

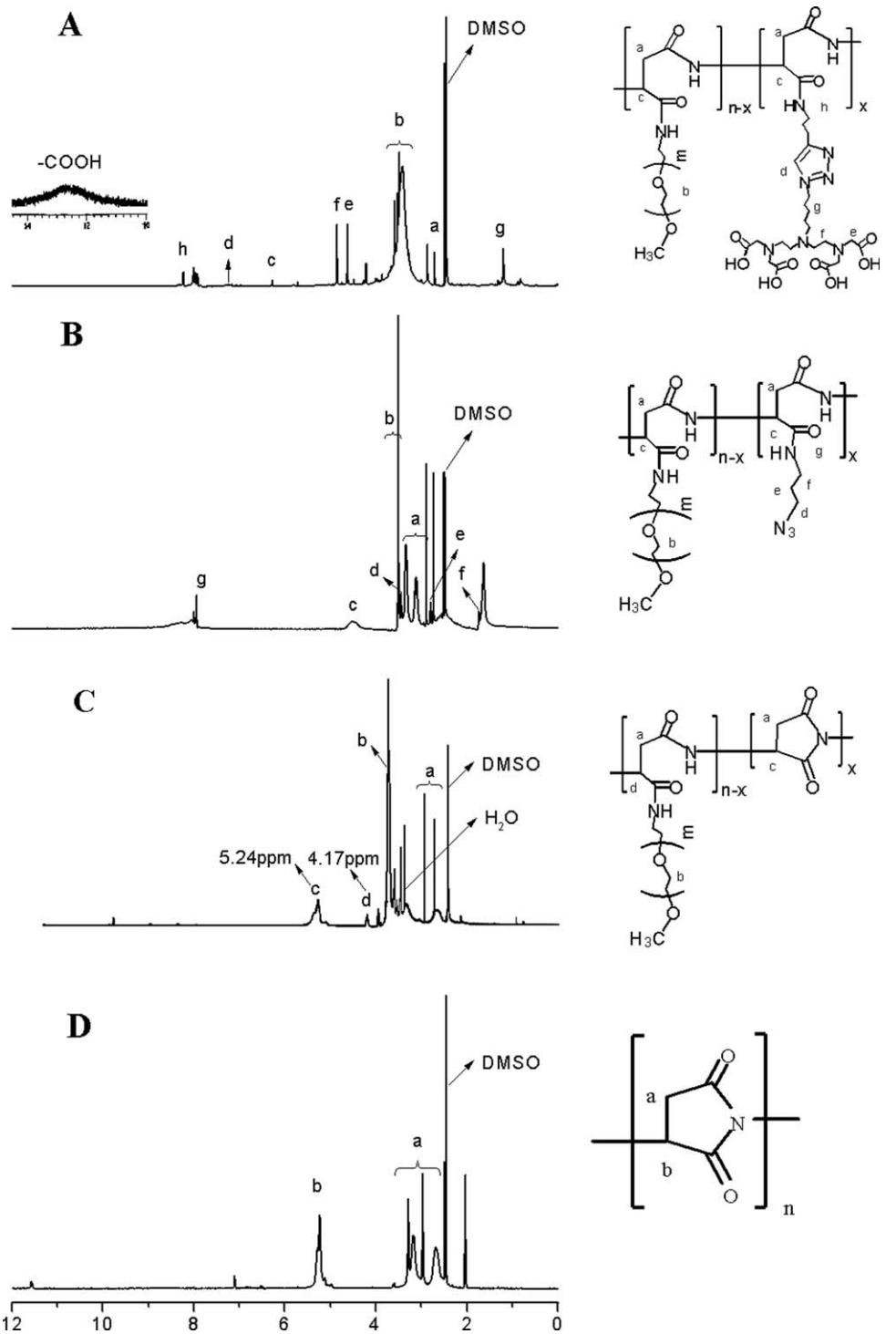

Figure 1 ^{1}H-NMR spectra of mPEG-*g*-PAA-DTTA (A), mPEG-*g*-PAA-N_3 (B), mPEG-*g*-PSI (C), and PSI (D) in d_6-DMSO. The very sharp peaks at 2.5 and 3.2 ppm correspond to DMSO and water, respectively.

After deprotection of carboxylic groups, mPEG-*g*-PAA-DTTA macromolecular ligands were obtained. The disappearance of the peak between 1.2 and 1.5 ppm assigned to *tert*-butyl ester (Bu^t) protons in DTTA-der indicated the successful deprotection of Bu^t groups (data not shown). The proton peak between 11 and 14 ppm [Fig. 1(A)] indicated the presence of carboxylic groups in mPEG-*g*-PAA-DTTA, which further confirmed the removal of Bu^t groups. The lyophilized mPEG-*g*-PAA-DTTA was a fluffy white solid with good water-soluble and hygroscopic nature. The mass percentage content of Gd in mPEG-*g*-PAA-(DTTA-Gd) (GD = 2%) measured by ICP-AES was 16.1%, similar to its theoretic value of 16.8% (Table II).

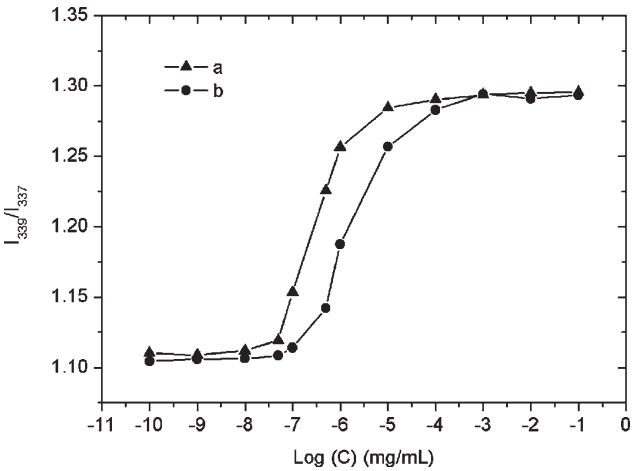

Figure 2 Plots of the ratio of I_{339}/I_{337} value from fluorescence spectra as a function of the concentration of complex nanomicelles: (a) mPEG-*g*-PAA-(DTTA-Gd) (GD = 7%), (b) mPEG-*g*-PAA-(DTTA-Gd) (GD = 2%). Pyrene was used as molecular probe ([Pyrene] = $6.0 \times 10^{-7}M$).

Complexation ratio of mPEG-g-PAA-(DTTA-Gd) was determined by FTIR spectroscopy (not shown) according to Buyuktas.[24] $GdCl_3$ was complexed with mPEG-*g*-PAA-DTTA in an equal molar ratio based on the FTIR results.

Micellization study of mPEG-*g*-PAA-(DTTA-Gd) complex

It was expected that the self-assembly of mPEG-*g*-PAA-(DTTA-Gd) complex produces nanomicelles in aqueous medium. In this case, the DTTA-Gd was sequestered toward the core of particle whereas the mPEG-*g*-PAA backbone forms the hydrophilic shell. To monitor the formation of mPEG-*g*-PAA-(DTTA-Gd) complex nanomicelles in aqueous media, CMC was measured by fluorescence spectrophotometer. Pyrene was used as probe to monitor the formation of the mPEG-*g*-PAA-(DTTA-Gd) nanomicelles in aqueous media. The I_{339}/I_{337} ratio in the excitation spectra of pyrene was shown to correlate well with solvent polarity according to previous method.[25] Thus, the ratio of I_{339}/I_{337} served as a measure of the polarity of micro-environment. As far as an amphiphilic polymer was concerned, when the concentration of the amphiphilic polymer reached the critical aggregation concentration, there is a major change for the I_{339}/I_{337} value. It was due to the transfer of pyrene from polar micro-environment to nonpolar micro-environment caused by the formation of micelles.

Figure 2 showed the curves of I_{339}/I_{337} versus concentrations of mPEG-*g*-PAA-(DTTA-Gd) polymeric complexes. As expected, mPEG-*g*-PAA-(DTTA-Gd) complexes were assembled into micelles due to the poor water-solubility of metal Gd ions after the complex formed between mPEG-*g*-PAA-DTTA and Gd. The CMC values of mPEG-*g*-PAA-(DTTA-Gd) (GD = 2%) and mPEG-*g*-PAA-(DTTA-Gd) (GD = 7%) were 1×10^{-6} and 1×10^{-7} mg/mL, respectively. The higher CMC value corresponding lower GD was attributed to the increased mass percentage of Gd in mPEG-*g*-PAA-(DTTA-Gd) complex.

TABLE I
Properties of the mPEG-*g*-PAA-DTTA Copolymers

Polymers	GD (%)[a]	($M_n \times 10^{-4}$)[b]	Polydispersity index[b]
mPEG-*g*-PAA-DTTA (GD = 2%)	1.8	3.24	1.32
mPEG-*g*-PAA-DTTA (GD = 7%)	6.6	3.76	1.35

[a] Determined by ^{1}H-NMR.
[b] Determined by Agilent 1200 GPC, PEG as standard samples.

Sizes, size distributions, and zeta potentials of mPEG-*g*-PAA-(DTTA-Gd) nanomicelles

As polymeric contrast complexes, the sizes of complexes assembled between polymers and Gd are known to dramatically affect the pharmacokinetics. The particle sizes and size distributions of mPEG-*g*-PAA-(DTTA-Gd) nanomicelles measured by DLS in an aqueous media were shown in Table I. The size distributions of all the micelles were narrow, their sizes were smaller than 100 nm, suggesting their efficient passive target potential to tumor tissue.[26] In addition, from Table II, the particle size of

TABLE II
Characteristics of mPEG-*g*-PAA-(DTTA-Gd) Complex Nanomicelles

Nanomicelles	Gd (%)[a]	ζ potential (mV)[b]	Hydrodynamic diameter (nm)[b]	PI[b]	CMC (mg/mL)[c]
mPEG-*g*-PAA-(DTTA-Gd) (GD = 2%)	16.1	−3.4	82	0.10	1×10^{-6}
mPEG-*g*-PAA-(DTTA-Gd) (GD = 7%)	12.2	−3.0	63	0.10	1×10^{-7}

[a] Determined by Inductively coupled plasma atomic emission spectroscopy.
[b] Polydispersity Index determined by dynamic light scattering.
[c] Determined by fluorescence probe method using pyrene as fluorescent probe.

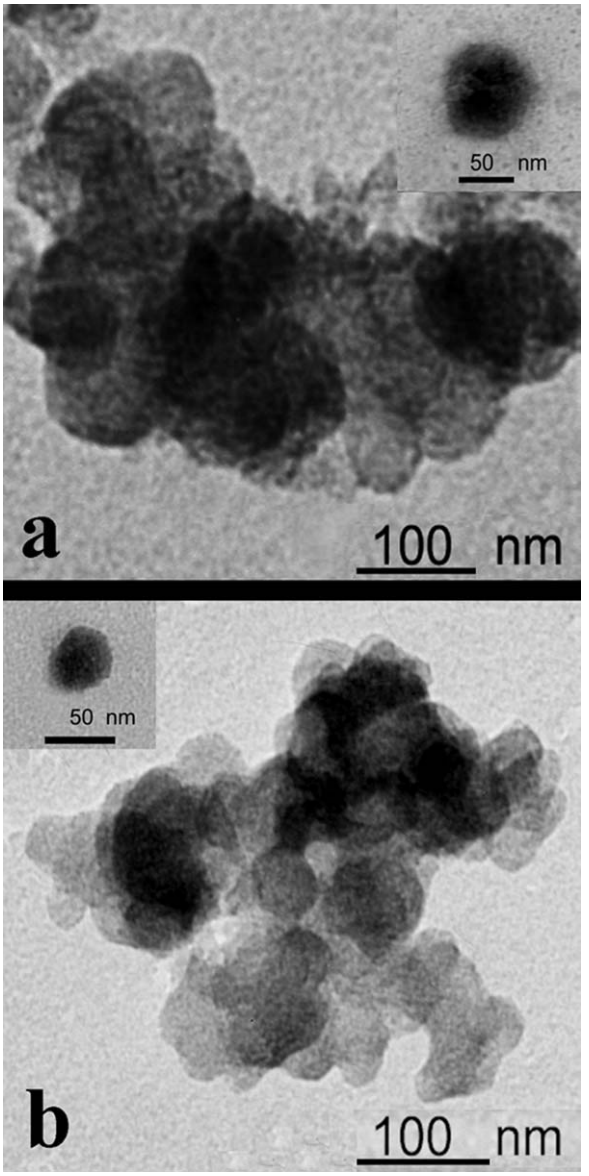

Figure 3 TEM photographs of polymeric nanomicelles: (a) mPEG-*g*-PAA-(DTTA-Gd) (GD = 2%); (b) mPEG-*g*-PAA-(DTTA-Gd) (GD = 7%).

mPEG-*g*-PAA-(DTTA-Gd) (GD = 2%) nanomicelles was larger than that of mPEG-*g*-PAA-(DTTA-Gd) (GD = 7%). According to the previous research results,[22] the increased PEG content obviously resulted in the increased steric repulsion of micelles between the hydrophilic coronas, which can be balanced out only by the increase in the curvature of the surface of the hydrophobic core. As shown in Table II, all the mPEG-*g*-PAA-(DTTA-Gd) nanomicelles showed negative zeta potentials.

Morphology observation of mPEG-*g*-PAA-(DTTA-Gd) nanomicelles

The morphologies of the complex nanomicelles of mPEG-*g*-PAA-(DTTA-Gd) were observed by TEM. The shape of complex nanomicelles was close to sphere, as seen in Figure 3. Because DTTA and Gd formed poor water-soluble complexes, it was expected that the self-assembling of mPEG-*g*-PAA-DTTA with Gd produced nanomicelles with core-shell structure, where DTTA-Gd was sequestered toward the micelle core and mPEG formed the hydrophilic shell. The hypothesis of core-shell nanomicelles was confirmed by the enlarged inserted figure, where the dark region was wrapped by the light corona. Sizes of mPEG-*g*-PAA-(DTTA-Gd) (GD = 2%) and mPEG-*g*-PAA-(DTTA-Gd) (GD = 7%) were 50 nm and 62 nm, respectively, smaller than those measured by DLS (Table II). The spherical shapes and good dispersity of nanomicelles were further confirmed by their typical AFM images (Fig. 4).

Cytotoxicity of mPEG-*g*-PAA-(DTTA-Gd) nanomicelles

In vitro cytotoxicity of mPEG-*g*-PAA-(DTTA-Gd) nanomicelles was evaluated with KB cell lines by MTT assay. Representative concentration-growth inhibition curves showing the effects of treatments with mPEG-*g*-PAA-(DTTA-Gd) micelles on the growth of KB after 24 h were shown in Figure 5. Although both mPEG-*g*-PAA-(DTTA-Gd) nanomicelles and Gd-DTPA inhibited cell growth in a dose-dependent manner, the former was consistently much less toxic than that of Gd-DTPA, especially at higher dose. The cell viability of mPEG-*g*-PAA-(DTTA-Gd) was above 85%, even after 24 h of incubation at a drug concentration of 200 μg/mL. Noticeably, at the same concentration, mPEG-*g*-PAA-(DTTA-Gd) (GD = 2%) < mPEG-*g*-PAA-(DTTA-Gd) (GD = 7%) was ranked according to their cell viabilities, suggesting that the increased GD resulted in the increase of its cytotoxicity, which were contributed to the increase of Gd content.

In vitro MRI contrast enhancement and relaxitivity

T_1-weighted MR images of the mPEG-*g*-PAA-(DTTA-Gd) were shown in Figure 6. T_1 is the value of spin-lattice relaxation time. In this image, when the concentration of Gd was above 0.5×10^{-3} M, the image contrast showed similar patterns, but when the concentration of Gd was below 0.5×10^{-3} M, the image contrast of mPEG-*g*-PAA-(DTTA-Gd) (GD = 2%) was better than that of mPEG-*g*-PAA-(DTTA-Gd) (GD = 7%). The result may be contributed to the higher gadolinium content in mPEG-*g*-PAA-(DTTA-Gd) (GD = 2%). Table III showed signal intensity values according to different concentrations of Gd. From these data, the

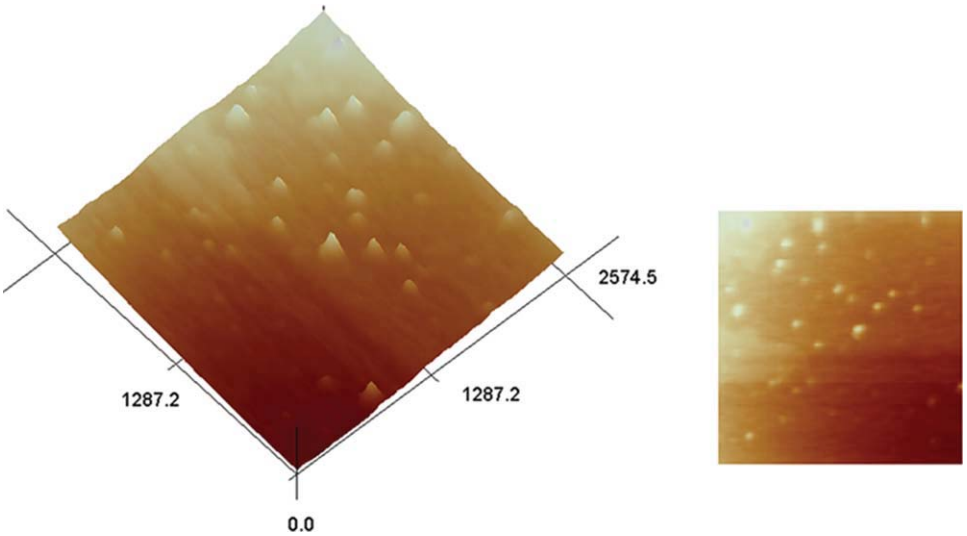

Figure 4 AFM image of mPEG-*g*-PAA-(DTTA-Gd) (GD = 2%) nanomicelle. [Color figure can be viewed in the online issue, which is available at wileyonlinelibrary.com.]

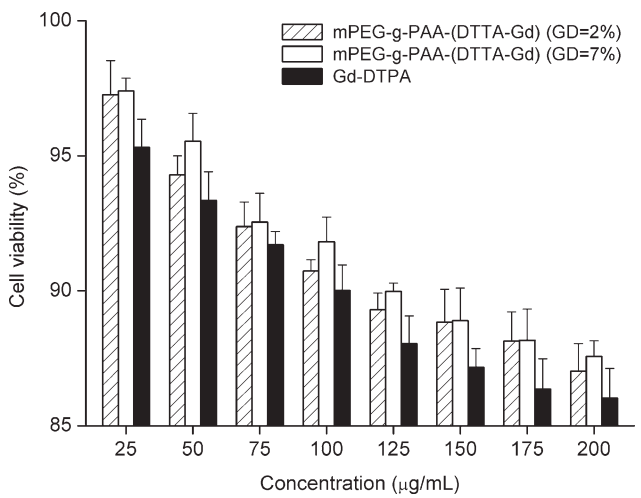

Figure 5 Cell viability of complex nanomicelles at various Gd concentration in KB for 24 h (mean ± SD, n = 3): (a) mPEG-*g*-PAA-(DTTA-Gd) (GD = 2%), (b) mPEG-*g*-PAA-(DTTA-Gd) (GD = 7%), and (c) Gd-DTPA.

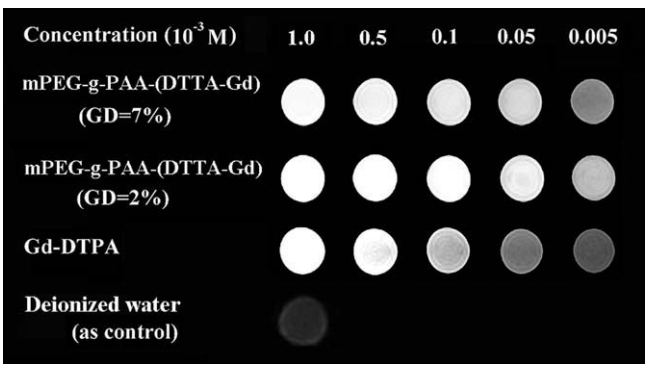

Figure 6 Contrast effect of mPEG-*g*-PAA-(DTTA-Gd) nanomicelles, Gd-DTPA and deionized water (as control) measured by MRI at 3.0 T, 10 MHz, 20°C.

signal intensity of mPEG-*g*-PAA-(DTTA-Gd) (GD = 2%) in 0.1×10^{-3} M similar to that of Gd-DTPA in 0.5×10^{-3} M indicated that the prepared samples had better contrast imaging at a lower concentration than that of Gd-DTPA. The results were contributed to the higher molecular weight of the prepared samples than Gd-DTPA, and also meant much lower dosage of mPEG-g-PAA-(DTTA-Gd) should be used for obtaining the same MR image in clinic application.

To know better the potentials of mPEG-g-PAA-(DTTA-Gd) as macromolecular MRI contrast agent, their relaxation rates were measured. Gd-DTPA was used as positive controls. The r_1 of mPEG-g-PAA-(DTTA-Gd) (GD = 2%) and mPEG-g-PAA-(DTTA-Gd) (GD = 7%) were 18.12 and 15.27 $mM^{-1}s^{-1}$, respectively, sharply higher than that of Gd-DTPA (4.68 mM^{-1} s^{-1}), suggesting of their potentials as macromolecular MRI contrast agents. With an increase of Gd content, the r_1 of mPEG-g-PAA-(DTTA-Gd) showed a tendency to increase.

TABLE III
Signal Intensity Values with Different Concentrations of Gd Measured by MRI

	Signal intensity		
Concentration of Gd (M)	Gd-DTPA	mPEG-*g*-PAA-(DTTA-Gd) (GD = 2%)	mPEG-*g*-PAA-(DTTA-Gd) (GD = 7%)
1.0×10^{-3}	1706.84	1819.87	1789.47
0.5×10^{-3}	1571.56	1657.31	1602.31
0.1×10^{-3}	1034.38	1570.03	1369.65
0.5×10^{-4}	708.42	1380.76	1030.16
0.5×10^{-5}	554.56	985.42	725.97

CONCLUSIONS

Core-shell mPEG-*g*-PAA-(DTTA-Gd) complex nanomicelles were fabricated from mPEG-*g*-PAA-DTTA and Gd ions. Their sizes measured by DLS were 50 to 80 nm, suggesting their passive targeting potential to tumor tissue. With the increase of GD of mPEG-*g*-PAA-(DTTA-Gd) nanomicelles, their size and CMC showed a tendency to increase. Compared with Gd-DTPA, mPEG-*g*-PAA-(DTTA-Gd) nanomicelles showed enhanced T_1-weighted signal intensity, higher relaxitivity, and remarkable decreased cytotoxicity, suggesting their great potential as MRI contrast agents.

References

1. Lauffer, R. E. Chem Rev 1987, 87, 901.
2. Rohrer, M.; Bauer, H.; Mintorovitch, J.; Requardt, M; Weinmann, H. J. Invest Radiol 2005, 40, 715.
3. Luo, Y.; Zhuo, R. X.; Shi, Y. T. World Pharm 1995, 16, 200.
4. Kim, J. H.; Park, K.; Nam, H. Y.; Lee, S.; Kim, K.; Kwon, I. C. Prog Polym Sci 2007, 32, 1031.
5. Doble, D. M. J.; Botta, M.; Wang, J.; Aime, S.; Barge, A.; Raymond, K. N. J. J Am Chem Soc 2001, 123, 10758.
6. Arebizak, R.; Schaefer, M.; Dellacherie, E. Bioconjugate Chem 1997, 8, 605.
7. Weissleder, R.; Bogdanov, A. Jr.; Tung, C. H.; Weinmann, H. J. Bioconjugate Chem 2001, 12, 213.
8. Ye, F. R.; Ke, T. Y.; Jeong, E. K.; Wang, X. L.; Sun, Y. E.; Johnson, M.; Lu, Z. R. Mol Pharmacol 2006, 3, 507.
9. Mohs, A. M.; Wang, X.; Goodrich, K. C.; Zong, Y.; Parker, D. L.; Lu, Z. R. Bioconjugate Chem 2004, 15, 1424.
10. Venditto, V. J.; Aida, C.; Brechbiel, M. W. Mol Pharmacol 2005, 2, 302.
11. Langereis, S.; De Lussanet, Q. G.; Van Genderen, M. H. P.; Backes, W. H.; Meijer, E. W. Macromolecules 2004, 37, 3084.
12. Barrett, T.; Kobayashi, H.; Brechbiel, M.; Choyke, P. L. Eur J Radiol 2006, 60, 353.
13. Blanco, E.; Kessinger, C. W.; Sumer, B. D.; Gao, J. Exp Biol Med (Maywood) 2009, 234, 123.
14. Nishiyama, N.; Kataoka, K. Pharmacol Ther 2006, 112, 630.
15. Huber, M. M.; Staubli, A. B.; Kustedjo, K.; Gray, M. H. B.; Shih, J.; Fraser, S. E.; Jacobs, R. E.; Meade, T. J. Bioconjugate Chem 1998, 9, 242.
16. Nishiyama, N.; Yokoyama, M.; Aoyagi, T.; Okano, T.; Sakurai, Y.; Kataoka, K. Langmuir 1999, 15, 377.
17. Wang, C. Y.; Gong, Y. B.; Fan, N. Q.; Liu, S. Y.; Luo, S. F.; Yu, J. H.; Huang, J. J. Colloids Surf B 2009, 70, 84.
18. Zalipsky, S.; Gilon, C.; Zilkha, A. Eur Polym J 1983, 19, 1177.
19. Carboni, B.; Benanlil, A.; Vaultier, M. J Org Chem 1993, 58, 3736.
20. Bryson, J. M.; Chu, W. J.; Lee, J. H.; Reineke, T. M. Bioconjugate Chem 2008, 19, 1505.
21. Zhao, Y.; Su, H. J.; Fang, L.; Tan, T. W. Polymer 2005, 46, 5368.
22. Chen, W.; Chen, H. R.; Hu, J. H.; Yang, W. L.; Wang, C. C. Colloids Surf A 2006, 278, 60.
23. Mynar, J. L.; Choi, T. L.; Yoshida, M.; Kim, V.; Hawker, C. J.; Fréchet, J. M. J. Chem Commun 2005, 41, 5169.
24. Buyuktas, B. S. Transition Met Chem 2006, 31, 786.
25. Amado, E.; Augsten, C.; Mäder, K.; Blume, A.; Kressler, J. Macromolecules 2006, 39, 9486.
26. Hirsch, L. R.; Gobin, A. M.; Lowery, A. R.; Tam, F.; Drezek, R. A.; Halas, N. J.; West, J. L. Ann Biomed Eng 2006, 34, 15.